Research Article

Citric Acid Production by *Aspergillus niger* in Stirred Tank Bioreactor

Kanjana Detchomphoo, Nicharee Wisuthiphaet and Sasithorn Kongruang*
Department of Biotechnology, Faculty of Applied Science, King Mongkut's University of Technology North Bangkok, Bangkok, Thailand

Rittipun Rungruang
Department of Cosmetic Science, Faculty of Science and Technology, Suan Dusit University, Bangkok, Thailand

* Corresponding author. E-mail: sasithorn.k@sci.kmutnb.ac.th DOI: 10.14416/j.asep.2025.08.002
Received: 27 April 2025; Revised: 31 May 2025; Accepted: 19 June 2025; Published online: 22 August 2025

Abstract
The optimization of citric acid production by submerged fermentation using *Aspergillus niger* TISTR 2365 was studied on upstream and downstream processing using a modified medium. The Box-Behnken Design was used for optimization, varying carbon to nitrogen ratios (70, 85, 100 g/L), shaking speed (200, 250, 300 rpm), and $CaCl_2$ supplementation (0.01, 0.055, 0.1 g/L) across 17 experimental runs. Batch fermentations were conducted in a 250 mL Erlenmeyer flask for 7 days at 30 °C. Results found the optimum citric acid was obtained at 27.73 g/L at a carbon to nitrogen ratio of 97.32 g/g, shaking speed of 300 rpm, and $CaCl_2$ supplementation of 0.10 g/L. Model validation of citric acid production of 25.43 g/L was confirmed in a 5-L stirred tank bioreactor, with an 8.29% deviation from the predicted value. Three operational runs in a bioreactor yielded citric acid concentrations of 26.88 g/L, 21.76 g/L, and 26.88 g/L, respectively. The highest citric acid yield was achieved in the third batch, reaching 0.25 g/g glucose, while the average yield from substrate utilization was approximately 0.20 g/g glucose. The results highlight the effectiveness of fermentation conditions and the role of $CaCl_2$ in enhancing citric acid production. Downstream processing was performed to purify the citric acid by the precipitation method. Purified citric acid was then quantified and analyzed by HPLC and FTIR.

Keywords: *Aspergillus niger*, Box-Behnken design, Citric acid, Fermentation, FTIR, Kinetics, SEM

1 Introduction

Aspergillus niger is a filamentous fungus belonging to the phylum *Ascomycota*, class *Eurotiomycetes*, and genus *Aspergillus* [1]. It is ubiquitously found in soil, decaying plant matter, and it is recognized as one of the most important microbial workhorses in industrial biotechnology. Its significance arises from its exceptional metabolic versatility, robust growth in acidic environments, and the ability to produce a broad spectrum of commercially valuable primary and secondary metabolites. Since the early 20th century, *A. niger* has been extensively utilized for large-scale fermentation, most notably for the industrial production of citric acid [2]–[4]. Today, *A. niger* remains the dominant microorganism for citric acid production globally, with industrial yields reaching millions of tons annually. Beyond citric acid, *A. niger* is also employed in the commercial production of numerous industrial enzymes, including glucoamylase, pectinase, cellulase, protease, lipase, phytase, catalase, and β-galactosidase [5]–[11]. These enzymes are widely used in sectors such as food and beverage, animal feed, detergents, textiles, and pharmaceuticals. Furthermore, *A. niger* produces a wide array of secondary metabolites, some of which possess pharmaceutical potential, such as the non-ribosomal peptide enniatin, while others, like ochratoxin A and fumonisin, are classified as mycotoxins and require careful regulation in industrial strains [2].

The metabolic potential of *A. niger* is predicated on its diverse and highly regulated metabolic pathways. Central to its biosynthetic capacity is the citric acid cycle (Krebs cycle), which can be manipulated

to favor citric acid accumulation rather than complete respiration. This is achieved through the regulation of enzyme activities, carbon source optimization, and control of environmental factors such as pH and aeration. In addition to the citric acid cycle, *A. niger* utilizes the pentose phosphate pathway (PPP) to generate NADPH, which is essential for anabolic biosynthesis and oxidative stress responses, as shown in Figure 1.

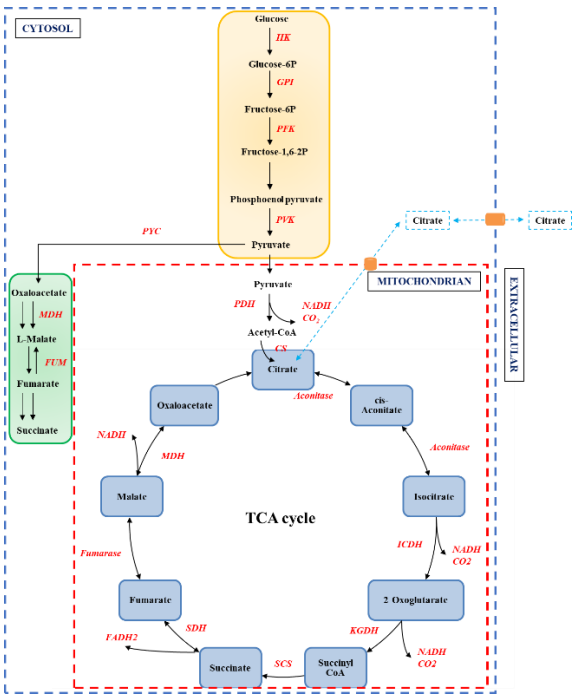

Figure 1: Metabolic pathway for organic acid production by *A. niger* using glucose as a substrate.

The synthesis of citric acid in fungi is a complex process that begins with glycolysis, followed by reactions in the tricarboxylic acid cycle (TCA cycle) within the mitochondria. Initially, glucose undergoes glycolysis in the cytoplasm, where the enzyme Hexokinase (HK) catalyzes the phosphorylation of glucose to form glucose-6-phosphate (Glucose-6P) using ATP [12]. Subsequently, Phosphoglucose Isomerase (GPI) converts glucose-6-phosphate into fructose-6-phosphate (Fructose-6P), which serves as the precursor for the next step. The enzyme Phosphofructokinase-1 (PFK-1) [13] then phosphorylates fructose-6-phosphate to form fructose-1,6-bisphosphate (Fructose-1,6-bisphosphate), utilizing ATP again, marking a critical control point in glycolysis [14]. Next, Pyruvate Kinase (PVK) completes the final step of glycolysis by converting fructose-1,6-bisphosphate into pyruvate (Pyruvate), generating ATP in the process. The resulting pyruvate is transported into the mitochondria, where it is converted into acetyl-CoA by the enzyme Pyruvate Dehydrogenase (PDH). This conversion releases CO_2 and produces NADH, which is crucial for subsequent energy production in the TCA cycle. With Acetyl-CoA now formed, it enters the TCA cycle where it participates in a series of reactions aimed at generating high-energy molecules, such as ATP, NADH, and $FADH_2$.

The first reaction of the TCA cycle involves Acetyl-CoA reacting with oxaloacetate and water, catalyzed by Citrate Synthase (CS), resulting in the formation of citrate, the starting point of the TCA cycle. In the second step, citrate undergoes dehydration to form cis-aconitic acid with the help of Cis-aconitase. This intermediate is then rehydrated to produce isocitric acid (Isocitrate) through the action of the same enzyme. In the third step, isocitric acid is oxidized to form α-ketoglutaric acid (α-Ketoglutarate) by Isocitrate Dehydrogenase (ICDH) [15], a reaction that produces NADH and releases CO_2. The fourth reaction involves α-ketoglutaric acid reacting with CoA to form succinyl-CoA, catalyzed by α-Ketoglutarate Dehydrogenase (KGDH). This step also releases CO_2 and generates NADH. The fifth step sees succinyl-CoA being converted to succinate through the release of energy, which is used to generate GTP, equivalent to ATP, catalyzed by Succinyl-CoA Synthase, with the addition of water. In the sixth step, succinate is oxidized by Succinate Dehydrogenase (SDH), producing $FADH_2$ and transforming succinate into fumaric acid (Fumarate). The seventh step involves the hydration of fumaric acid to form malic acid (Malate), catalyzed by Fumarase. Finally, in the eighth step, malic acid loses 2H to NAD+, resulting in the formation of NADH and regenerating oxaloacetate (Oxaloacetate) through the action of Malate Dehydrogenase (MDH). The production of oxaloacetate in this step completes the TCA cycle, enabling it to begin again by combining with acetyl-CoA.

The synthesis and transport of citrate out of the mitochondria is a critical process in maintaining the efficiency of the TCA cycle. The Tricarboxylate Transporter (MTT) facilitates the exchange of citrate with malate or succinate, enabling the transfer of citrate from the mitochondria to the cytoplasm. This transport is regulated by manganese (Mn^{2+}) levels and the intracellular pH [16], ensuring the proper flow of metabolites through the TCA cycle and facilitating continued cellular respiration and energy production.

Several factors, including the type and concentration of carbon sources, nitrogen and phosphate limitations, pH, aeration, trace metal concentrations, and the morphology of the producing microorganism, significantly influence citric acid yield. Optimal production conditions require certain nutrients, such as sugars, protons, and oxygen, to be provided in excess, while nitrogen and phosphate must be maintained at limiting levels [17], [18]. Additionally, trace metals like manganese should be kept below certain thresholds to avoid inhibitory effects [19], [20]. Building on these early findings, more recent studies have focused on the effects of various fermentation parameters. Hossain *et al*., [20] investigated citric acid production from *A.niger* in a 6-liter fermenter with an initial air flow rate of 3 L/min, which increased to 5 L/min after 48 h. They observed that sucrose as a carbon source led to a higher citric acid yield (38 g/L) compared to glucose (13 g/L), with sucrose also showing a higher productivity of 34 mg/g dry weight per hour. Similarly, Papagianni *et al*., [21] studied citric acid production in batch and fed-batch cultures using glucose as the carbon source; higher agitation speeds (600 rpm) resulted in increased citric acid production (125 g/L) compared to lower speeds (200 rpm, 58 g/L). The study further demonstrated that lower glucose concentrations (17 g/L) in fed-batch cultures resulted in higher vacuolation levels and reduced production rates, emphasizing the importance of maintaining optimal glucose levels for maximizing productivity. Yin *et al*., [22] examined citric acid production using *A.niger* H915-1 under fed-batch conditions with a 3-liter fermenter, achieving a maximum citric acid yield of 157 g/L in 85 h with a volumetric productivity of 2.79 g/L/h. These studies collectively highlight the complex interplay of fermentation conditions, medium composition, and microbial morphology, all of which contribute to the optimization of citric acid production in industrial fermentation processes.

From the studies by Hossain *et al*. and Yin *et al*. [20]–[22], the relationship between fermentation conditions and the physical characteristics of microorganisms was examined, similarly to the work of Papagianni *et al*. [21], who investigated the effects of high agitation speed (600 rpm) on the morphology of *A.niger* mycelium and its subsequent impact on citric acid production. Their study revealed that high agitation speeds led to the formation of shorter, thicker hyphal filaments with fewer vacuoles, which were associated with increased citric acid production compared to lower agitation speed (200 rpm). Excessive agitation can cause fragmentation, leading to reduced productivity, while insufficient agitation may result in large clumps that hinder oxygen diffusion. Intense agitation caused hyphal fragmentation. High agitation rates can impose shear stress on fungal cells, potentially damaging them and negatively affecting citric acid yield [21].

In contrast, lower agitation speeds resulted in increased vacuolation, which weakened the hyphae and reduced biosynthetic activity, leading to a decrease in citric acid production. These findings highlight the importance of optimizing agitation speed to enhance citric acid production in submerged fermentation. Building on these insights, our study further optimized citric acid production using a Box-Behnken Design to examine three key factors: the carbon-to-nitrogen (C/N) ratio, shaking speed, and $CaCl_2$ supplementation in Erlenmeyer flasks. This experimental approach aimed to preserve mycelial integrity while maximizing citric acid yield. The optimal shake-flask conditions were then applied to validate citric acid yield and productivity in a 5L stirred-tank bioreactor. To assess the effects of these variables on mycelium preservation, scanning electron microscopy (SEM) was utilized throughout the experiments. The results provided valuable insights into how morphological optimization, combined with process parameter adjustments, can enhance citric acid production while maintaining mycelial viability. These findings were critical for scaling up fermentation to a stirred-tank bioreactor, presenting a comprehensive strategy for improving citric acid productivity in pilot-scale processes.

2 Materials and Methods

2.1 *Microorganism and inoculum*

A. niger TISTR 2365 was obtained from the Thailand Institute of Scientific and Technological Research (Pathumthani, Thailand). Fungal strain was inoculated into an Erlenmeyer flask containing 100 mL of Potato Dextrose Broth (PDB) and maintained at 4 °C for stock cultures.

2.1.1 Inoculum preparation

A. niger TISTR 2365 from stock cultures was transferred to a sterile plate containing Potato Dextrose Agar (PDA). The cultures were incubated at 30 °C in a control incubator (Shaker Incubator, INC 125 FS digital, IKA-Werke GmbH & Co. KG., Staufen Germany).

After 168 h, the cultures were used as inoculum for batch cultivations in a shake flask.

2.1.2 Starter preparation of A.niger

The PDA-cultured *A. niger* was prepared by correctly suspending the spores from the mycelium growth in the PDB. The spore suspension of *A. niger* was prepared in sterile Tween 80 to a final concentration of 3×10^8 spores/mL using a Thomas hemacytometer.

2.2 *Morphological characteristics identification*

Each activated pure culture *A. niger* TISTR 2365 grown on PDA was smeared on a slide and identified the morphological characteristics on a light microscope with magnifications of 10, 40, and 100x.

2.3 *Phylogenetic tree analysis*

A nucleotide BLAST aligment for classification from National Center for Biotechnology Information (NCBI) was used to identify a set of homologous sequence of citric acid producing fungi from the following strains *A.niger* LC573607, *A. aculeatus* LC573562, *A. carbonarius* LC573579, *A. awamori* LC573570, *A. foetidus* LC573587, *A. phoenicis* LC573613, *A. luchensis* LC573598, *A. wentii* OW984456, *Penicillium janthinellum* MK450697, *P. janthinellum* AB293968, *P. purpurogenum* GU566251, *P. restrictum* KP016816, *P. citrinum* OW985441, *Trichoderma viride* LC535970 by using *Yarrowia lipolytica* AB018158 as a outgroup species. Phylogenetic analysis was conducted with MEGA11 (molecular evolutionary genetics analysis using maximum likelihood, evolutionary distance and maximum parsimony methods [23]. The phylogenic tree was constructed of a phylogenetic tree from the aligned sequences.

2.4 *Optimization of citric acid production*

The chosen parameters of citric acid production by free cell, *A. niger* TISTR 2365, were evaluated using response surface methodology (RSM). The Box-Behnken Design (BBD) with 3 factors and 3 levels was carried out statistical model for the individual and interactive effects of carbon to nitrogen ratio (70, 85, 100 g/g), shaking speed (200, 250, 300 rpm) and $CaCl_2$ (0.055, 0.01, 0.1 g/L). Levels of these factors were optimized for maximum citric acid production (the response) according to Table 1. All the 17-trial experiments were investigated as Table 2. Four different polynomial models were tested as possible regression models for the data, namely, a linear model, a 2FI model, a quadratic model and a cubic model before the chosen model. The citric acid production could be modeled with a quadratic model by Equation (1) of the following form:

$$y_1 = \beta_0 + \sum_{i=1}^{4} \beta_i X_i + \sum_{i=1}^{4} \sum_{j=1}^{4} \beta_{ij} X_i X_j + \sum_{i=1}^{4} \beta_{ii} X_i^2 \quad (1)$$

Here, X_1, X_2, X_3 are the parameter values for the independent variables (carbon to nitrogen ratio, shaking speed, $CaCl_2$) as described in Table 2. The constants β_0, β_i, and β_{ij} (i, j = 1, 2, 3) are coefficient estimates for citric acid production(y_1), where β_0 is an intercept term, β_i are linear terms, β_{ii} are quadratic terms, and β_{ij} are interaction terms.

Table 1: Levels for each factor that affects the efficiency of citric acid production by *A.niger*.

Factor	Level			Unit
	-1	0	1	
A: Carbon to Nitrogen ratio	70	85	100	(g/g)
B: Shaking Speed	200	250	300	(rpm)
C: $CaCl_2$	0.01	0.055	0.1	(g/L)

Table 2: Levels of factors affecting total citric acid production.

Run	Factor 1 A:C/N (g/g)	Factor 2 B:Shaking Speed (rpm)	Factor 3 C:$CaCl_2$ (g/L)
1	70	300	0.055
2	85	200	0.1
3	100	300	0.055
4	85	250	0.055
5	100	250	0.01
6	70	200	0.055
7	85	250	0.055
8	70	250	0.01
9	100	200	0.055
10	100	250	0.1
11	85	200	0.01
12	70	250	0.1
13	85	300	0.1
14	85	250	0.055
15	85	250	0.055
16	85	250	0.055
17	85	300	0.01

The accuracy and general suitability of the above polynomial model could be evaluated by the coefficient of determination (R^2). The experimental data were analyzed using the statistical software, Design-Expert software version 10.0.6 (STAT-EASE Inc., Minneapolis, MN, USA), to carry out a regression

analysis for the equations and for an evaluation of the statistical significance. The data produced were analyzed to determine the optimum condition for citric acid production through F-value, R^2, p-value, residual error, pure error and lack of fit.

2.4.1 Media composition

The medium consisted of glucose ($C_6H_{12}O_6$) at concentrations of 70, 85, and 100 g/L, along with KH_2PO_4 (0.3 g/L), K_2HPO_4 (0.3 g/L), and $MgSO_4 \cdot 7H_2O$ (0.3 g/L). Urea was used as the nitrogen source to adjust the carbon-to-nitrogen (C/N) ratio to 70, 85, and 100 g/g, while three concentrations of $CaCl_2$ (0.01, 0.05, and 0.1 g/L) were incorporated. The pH of the medium was adjusted to 4 using hydrochloric acid, and the medium was sterilized at 121 °C for 15 min. After inoculation with 10% inoculum, 1% $CaCO_3$ was added following a 12-hour fermentation period. The fermentation was carried out in a shaking incubator at three different agitation speeds (200, 250, and 300 rpm) for six days at 30 °C.

2.5 *Analytical measurement*

Fermentations were performed in triplicate. Samples were withdrawn at the end of the fermentation period. The broth culture was centrifuged at 15,000 rpm to separate the mycelia. The collected filtrate was used to estimate residual sugar and citric acid production. The dry weight of mycelium was obtained by filtering broth samples through pre-weighed filter discs. Biomass concentration was determined by dry weight measurement. The harvested biomass was washed with 0.85% saline solution, followed by deionized water, then dried overnight at 105 °C, cooled in a desiccator, and weighed. Sugar concentration was measured using the dinitrosalicylic acid (DNS) method [24], while citric acid was quantified by titration with 0.1 N sodium hydroxide using phenolphthalein as an indicator [25]. The volume change of the sample solution from colorless to pink to red was recorded, calculated, and reported as the citric acid concentration.

2.6 *Scanning electron microscopy (SEM)*

Morphological characteristics of *A. niger* under different culture conditions**.** To study the changes in mycelium and its characteristics under different culture conditions, the samples were observed using SEM. For the fixed samples on the stump, a scanning electron microscope (JEOL JSM-IT500HR, Japan) with an accelerating voltage of 3.0 kV to 5.0 kV was used. The SEM images of the samples were recorded at 1000x, 2000x and 5000x magnifications [26].

2.7 *Validation of optimization modified media for citric acid production in a bioreactor*

2.7.1 Preparation of medium in the batch bioreactor

A modified liquid culture medium composed of 97 g of D-glucose, 1 g of urea, 0.3 g of KH_2PO_4, 0.3 g of K_2HPO_4, 0.3 g of $MgSO_4 \cdot 7H_2O$, 0.1 g/L of $CaCl_2$, and 1 g of $CaCO_3$ and pH 4 was prepared and transferred into a batch bioreactor with a working volume of 3 L. The medium was sterilized by autoclaving at 121 °C for 15 min at 15 lb/in^2 to ensure aseptic conditions before inoculation.

Figure 2: Citric acid production in a 5 L bioreactor using *A.niger* grown in modified media (A) 0-day of fermentation time.

2.7.2 Citric acid production in the batch bioreactor

The bioreactor system was assembled in accordance with the manufacturer's guidelines and connected to all necessary operational equipment. The fungal inoculum was prepared following the procedure outlined in Section 2.1.2, using the optimized culture conditions described in Section 2.4.1. To ensure reproducibility and reliability of the results, the fermentation process was carried out in triplicate. A volume of 300 mL of fungal pre-culture was inoculated into the 5 L batch bioreactor containing 3 L of sterilized liquid medium in the bioreactor (MDFT-N-5L, B.E. MARUBISHI CO., LTD., Bangkok Thailand) according to the setup in Figure 2. The

cultivation was initiated under the specified conditions: agitation speed of 300 rpm with 1L/min aeration rate at 30 °C, and sampling was performed every 48 h. Each sample, with a volume of 50 mL, was collected over a total cultivation period of 336 hours to monitor fungal growth kinetics and citric acid production.

2.8 *Downstream processing*

Citric acid precipitation was experimented by the precipitation method [27]. A 100 mL of fermentation broth was prepared, and the pH was adjusted using a 10% (w/v) NaOH solution. The NaOH solution was added dropwise and slowly while continuously stirring the mixture until the pH reached 8 or 9. This was indicated by a color change from yellow to orange, signifying the transition from an acidic to a neutral pH. Next, a 20% (w/v) calcium chloride ($CaCl_2$) solution was prepared and gradually added to the sodium citrate solution in the beaker. The mixture was stirred using a glass stirring rod to facilitate the reaction. The solution was heated to the boiling point. As the temperature increased, a white precipitate of calcium dicitrate formed. The precipitate was then recovered by vacuum filtration, washed with hot water three times and transferred to a beaker. A 10% (w/v) dilute sulfuric acid (H_2SO_4) solution was slowly added to the calcium dicitrate precipitate while stirring with a glass rod. The obtained citric acid was subjected to characterization with FTIR analysis.

2.9 *Characterization of citric acid*

2.9.1 Fourier Transform Infrared Spectroscopy (FT-IR Analysis)

The citric acid precipitate obtained from the fermentation broth was subjected to chemical composition analysis using Fourier Transform Infrared Spectroscopy (FT-IR) (Tensor 27, Bruker, Germany). The FT-IR spectrum of the citric acid sample was compared with that of commercial citric acid (Sisco Research Laboratories, India) and food-grade citric acid (Tokyo Chemical Industry, India). The analysis was conducted over a frequency range of 400–4000 cm^{-1}.

2.9.2 High-Performance Liquid Chromatography (HPLC)

2.9.2.1 Reagents

Sulfuric acid (98% analytical grade), methanol (99.96% analytical grade), citric acid HPLC standards were provided by Merck (USA). The mobile phase and sample preparation used deionized water, obtained from a Synergy® water purification system.

2.9.2.2 HPLC system and method validation

The quantification of citric acid from fermentation broth was carried out in an HPLC Prominence (Shimadzu Corporation, USA) controlled by a workstation with Lab Solutions software and, equipped with a UV/VIS diode array detector- DAD at 210 nm. IC-Pak Ion-Exclusion 7µm (7.8 × 300 mm) (Waters, USA) column at 40 °C was used for HPLC analyses with an isocratic mode at a flow rate of 0.6 mL/min and an injection volume of 10 µL. For method optimization, the mobile phase (sulfuric acid) was tested at concentrations ranging from 0.001 to 0.1N. A serial dilution of citric and oxalic acid was used for the construction of the calibration curve. The filtered standards were analyzed in triplicate for calibration, using an HPLC System. The validation parameters consider linearity range, precision, accuracy, detection and quantification limits. The peaks were identified by their retention times, comparing the UV-visible spectra and spiking with standards. Precision and accuracy were determined using the mean of consecutive injections of standard mixtures of citric and oxalic acid at different concentration levels, considering the relative standard deviation (%RSD).

2.9.3 Statistical analysis

The results from the study were expressed as mean ± standard deviation of three parallel measurements. The significance of difference was calculated by ANOVA using Design Expert version 13 with LSD and values p-value < 0.05, p < 0.01 and p-value < 0.001 were considered to be highly significant.

3 Results and Discussion

3.1 *Morphological characteristics of a citric acid-producing microorganism*

The fungus *A. niger* TISTR 2365, cultivated on Potato Dextrose Agar (PDA), demonstrated typical mycelial growth and the formation of black conidia, as observed in Figure 3. Colonies of *A. niger* initially appeared white but gradually turn black due to conidial maturation. They had a velvety or powdery

texture (Figure 3(a)). Both vegetative and aerial mycelia, along with conidiophores, were identified in the central region of the culture under microscopic examination, as shown in Figure 3(b) and (c). The conidiophores arose from the mycelium. They were long, unbranched, and terminated in a flask-shaped vesicle. To further understand the phylogenetic relationship of this strain, a multiple sequence alignment was performed using the query sequence as a tool for the analysis.

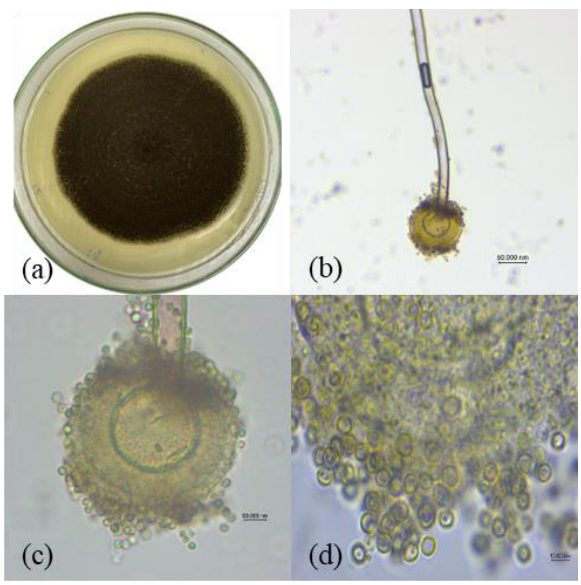

Figure 3: Morphological characteristics of *A. niger* (a) grown on PDA, (b) light microscope with magnification of 10x, (c) 40x, (d) 100x.

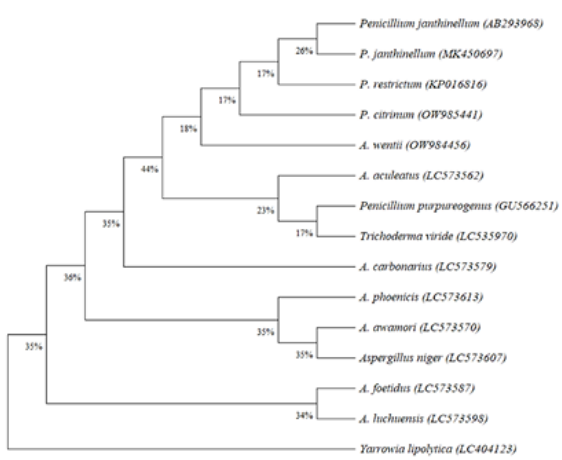

Figure 4: Phylogenetic tree from the aligned sequences to classify citric fermenting fungi.

3.2 *Phylogenetic tree of fungi*

A. niger exhibits significant global distribution and was noted for its phenotypic diversity. This widespread presence was partly due to its industrial application as a cell factory for citric acid production. Moreover, this strain had been extensively studied for its ability to efficiently produce commercial enzymes, including amylases, pectinases, and xylanases, in addition to its capacity for high organic acid consumption, particularly citric acid. The phylogenetic analysis also revealed that *A. niger* (LC573607) shares a close relationship with the conserved sequence of *A. phoenicis* (LC573613). This comparison was based on conserved nucleotide sequences analyzed through BLAST alignment, which identifies homologous regions among fungal species. The resulting evolutionary tree, shown in Figure 4, illustrates the hierarchical clustering of related organisms. Species with high genetic similarity are positioned closer together, reflecting shared evolutionary pathways. Such phylogenetic insights help clarify the genetic linkage of *A. niger*, informing studies on strain improvement and metabolic optimization for enhanced industrial applications.

3.3 *Optimization of citric acid production*

The optimization of citric acid production through fermentation by *A. niger* TISTR 2365 was systematically studied by adjusting various parameters in the modified fermentation medium. Citric acid concentration and yield from the fermentation process were recorded, as presented in Table 3.

To better understand the relationship between input variables and citric acid production, before the purification method of citric acid through the precipitation method, as illustrated in Figure 5, a quadratic model was derived from the experimental data, with the model's adequacy assessed through an Analysis of Variance (ANOVA). The model showed a high R-squared value of 0.9652, indicating that approximately 96.52% of the variability in the observed data could be accounted for by the model, suggesting a strong fit. The derived equation provides a more detailed understanding of how the experimental variables interact to influence citric acid production. Notably, the fermentation yield was found to be significantly influenced by the shaking speed (p = 0.0489) and the concentration of $CaCl_2$ (p-value = 0.0084), with citric acid yields ranging from 18.77 to

27.73 g/L. The interactive effects of these input variables were visualized through response surface graphs shown in Figures 6(a) to 7(c), all of which exhibited concave shapes, indicating that the optimal conditions for citric acid production lay within the defined parameter window. For instance, Figure 6(a) demonstrates that the interaction between the substrate concentration (C/N ratio) and shaking speed led to peak citric acid production of 27.73 g/L at the median values of these parameters. Further analysis revealed that the interaction between $CaCl_2$ concentration and the C/N ratio also resulted in the highest citric acid yield of 27.73 g/L at a shaking speed of 250 rpm, as shown in Figure 6(a). Additionally, Figure 6(b) illustrated that maintaining a C/N ratio of 85 and increasing the $CaCl_2$ concentration from 0.01% to 0.1% resulted in higher citric acid yields. The relationship between shaking speed, $CaCl_2$ concentration, and citric acid production was also explored in Figure 6c, which demonstrated how changes in these variables contributed to variations in citric acid yield. These findings highlight the complex interplay between the input parameters in optimizing citric acid production through fermentation.

Table 3: Box Benhken Design for the citric acid production and yield of *A. niger* fermentation.

Run	Factor 1	Factor 2	Factor 3	Response 1	Response 2
	A: C/N	B: Shaking Speed	C: $CaCl_2$	Citric acid	Yield
	(g/g)	(rpm)	(g/L)	(g/L)	(g/g)
1	70	300	0.055	18.77	0.76
2	85	200	0.1	21.33	0.52
3	100	300	0.055	27.73	0.51
4	85	250	0.055	22.61	0.51
5	100	250	0.01	23.04	0.4
6	70	200	0.055	19.63	0.68
7	85	250	0.055	22.19	0.5
8	70	250	0.01	20.91	0.7
9	100	200	0.055	23.04	0.42
10	100	250	0.1	25.6	0.44
11	85	200	0.01	22.19	0.52
12	70	250	0.1	19.63	0.68
13	85	300	0.1	23.04	0.59
14	85	250	0.055	22.61	0.53
15	85	250	0.055	22.61	0.52
16	85	250	0.055	22.61	0.52
17	85	300	0.01	21.33	0.52

The yield model derived from the experimental data demonstrated a high degree of accuracy, with an R-squared value of 0.9866, indicating that 98.66% of the variation in citric acid yield could be explained by the model. The statistical significance of the model was confirmed by a low *p*-value (<0.0001).

Experimental results indicated that citric acid yield was significantly influenced by the C/N ratio and shaking speed, with *p*-values of 0.0005 and 0.0314, respectively. The variation in citric acid yield ranged from 0.40 to 0.76 g/L. Figure 7(a) to (c) illustrate the interaction effects of these process parameters on citric acid formation. All graphs exhibited concave patterns, suggesting that optimal production conditions lie within the tested experimental range. Specifically, Figure 7(a) shows that a C/N ratio of 70 g/L glucose and a shaking speed of 300 rpm, supplemented with 0.055 g/L of $CaCl_2$, resulted in a peak citric acid yield of approximately 0.76 g/g. Similar interaction trends were observed at a shaking speed of 250 rpm, where variations in the C/N ratio and $CaCl_2$ concentration led to a maximum yield of approximately 0.76 g/g, as depicted in Figure 7(b) and (c). The mathematical relationships governing citric acid yield and productivity are expressed in Equations (2) and (3), which incorporate the effects of the carbon-to-nitrogen (C/N) ratio, shaking speed, and $CaCl_2$ supplementation, along with their interactions, to predict citric acid yield. These models provide valuable insights into the role of these parameters and their optimization in submerged fermentation, guiding further improvements in citric acid production efficiency.

$$\text{Citric acid} = 47.29 - 0.15 \times \text{C/N} - 0.18 \times \text{Shaking Speed} - 217.18 \times CaCl_2 + 1.85E\text{-}003 \times \text{C/N} \times \text{Shaking Speed} + 2.12 \times \text{C/N} \times CaCl_2 + 0.29 \times \text{Shaking Speed} \times CaCl_2 - 1.36E\text{-}003 \times \text{C/N}^2 + 2.92E\text{-}005 \times \text{Shaking Speed}^2 - 309.33 \times CaCl_2^2 \quad (2)$$

$$\text{Yield} = 3.57 - 0.05 \times \text{C/N} - 5.82E\text{-}003 \times \text{Shaking Speed} - 2.62 \times CaCl_2 + 3.33E\text{-}006 \times \text{C/N} \times \text{Shaking Speed} + 0.02 \times \text{C/N} \times CaCl_2 + 7.78E\text{-}003 \times \text{Shaking Speed} \times CaCl_2 + 2.09E\text{-}004 \times (\text{C/N})^2 + 1.14E\text{-}005 \times \text{Shaking Speed}^2 - 3.88 \times CaCl_2^2 \quad (3)$$

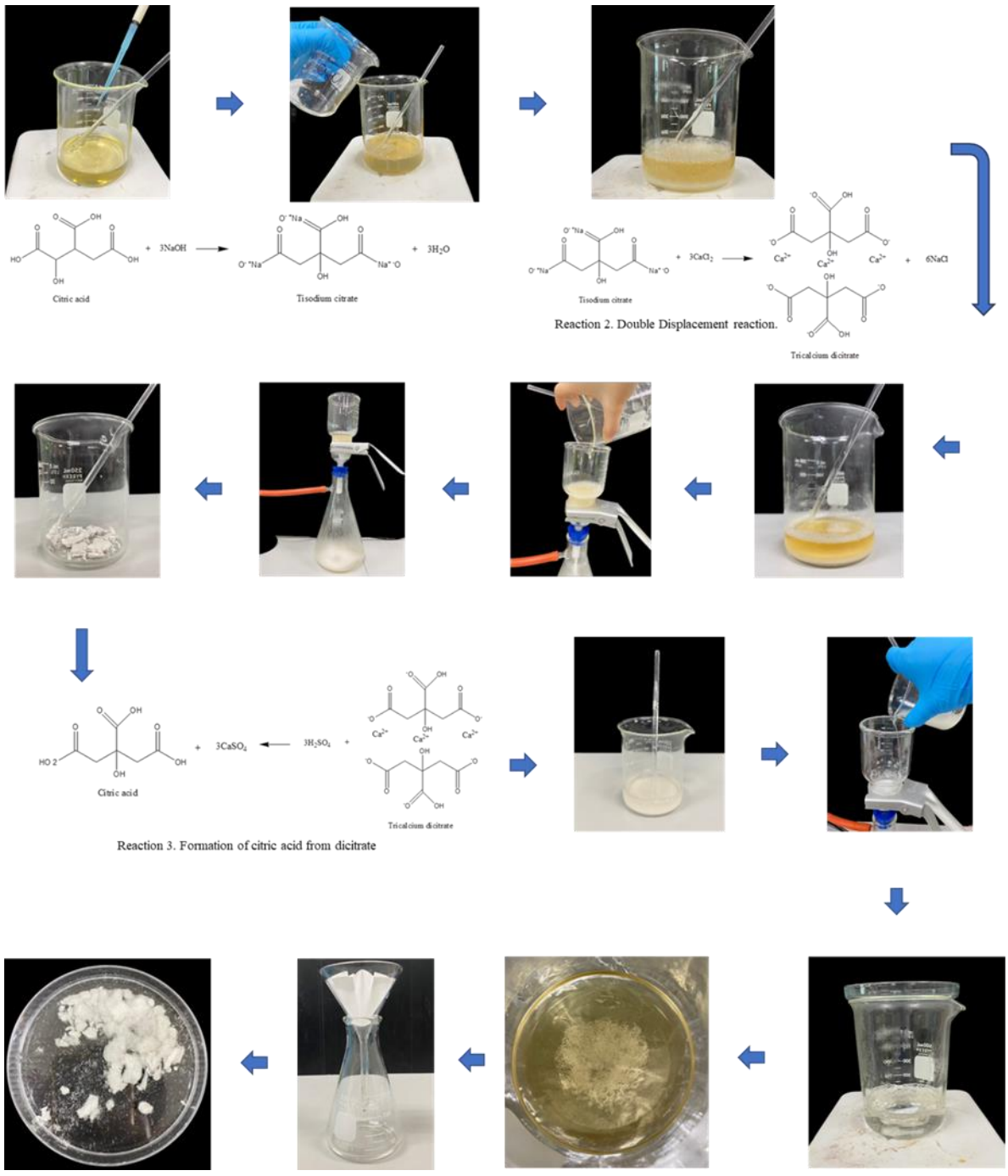

Figure 5: Recovery and purification of citric acid through the precipitation method.

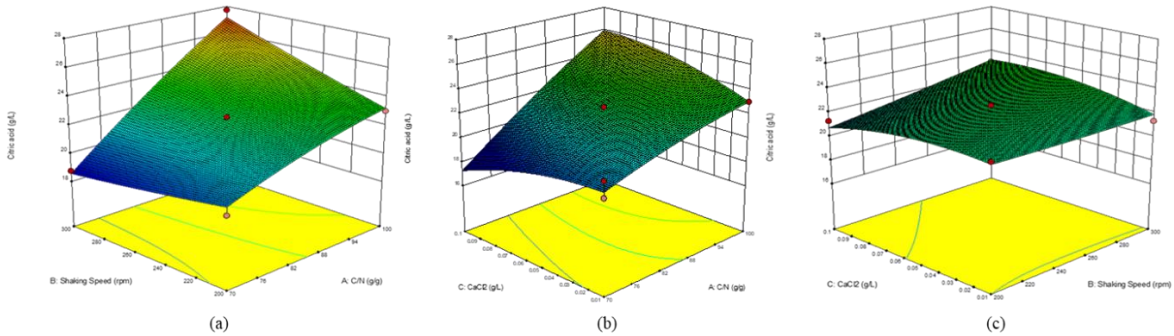

Figure 6: Response surface 3D graph of citric acid production (a) the effect of C/N ratio and shaking speed, (b) the effect of C/N ratio and $CaCl_2$, (c) shaking speed and $CaCl_2$.

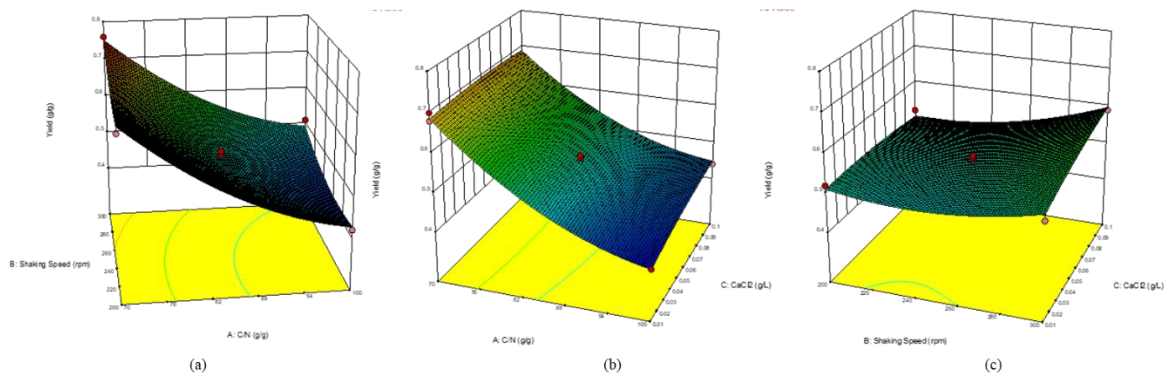

Figure 7: Response surface 3D graph for yield (a) by function of different C/N ratio and shaking speed, (b) the effect of C/N ratio and $CaCl_2$, (c) shaking speed and $CaCl_2$.

3.4 *Validation of optimization of the box-behnken design in a shake flask*

To validate the statistical optimization of citric acid production and yield using response surface design, a series of validation experiments were conducted to confirm the adequacy and accuracy of the model. The experiments were performed with modified media in shake flasks at a C/N ratio of 97 g/g in 100 mL. The media composition (g/L) included 97 g of D-glucose, 1 g of urea, 0.3 g of KH_2PO_4, 0.3 g of K_2HPO_4, 0.3 g of $MgSO_4 \cdot 7H_2O$, 0.1 g/L of $CaCl_2$, and 1 g of $CaCO_3$. These experiments were carried out in triplicate at 30 °C, pH 4, and 300 rpm over a period of 6 days of fermentation. The results of the validation experiments, performed under the optimum conditions, showed a high degree of agreement with the predicted citric acid production of 25.43 g/L, compared to the model prediction value of 27.73 g/L. The difference between the predicted and experimental values was 8.29%, which is less than 10%, demonstrating the validity and accuracy of the response surface model. This validation confirms that the model provides reliable results, supporting its use in optimizing the cultivation conditions and yield for citric acid production.

3.5 *Scale up the optimization condition in the bioreactor*

The optimization of citric acid production was then carried out in a stirred tank bioreactor using the desirability function to maximize the yield within the selected parameter ranges for the free cell of *A.niger* TISTR 2365 strain. These experiments were performed with modified media of a C/N ratio of 97 g/g, using a 3 L working volume in a stirred tank bioreactor. The media composition included 97 g of D-glucose, 1 g of urea, 0.3 g of KH_2PO_4, 0.3 g of K_2HPO_4, 0.3 g of $MgSO_4 \cdot 7H_2O$, 0.1 g/L of $CaCl_2$, and 1 g of $CaCO_3$. Experiments were carried out in a bioreactor at 30 °C, pH 4, and 300 rpm over 6 days of fermentation time as illustrated in Figure 8. The validation of the model was performed under the optimized conditions.

Figure 8: Citric acid production in a 5 L bioreactor using *A.niger* grown in modified media 6-day of fermentation time.

The results from the bioreactor fermentation experiment showed the characteristics of biomass and cell growth, with no damage observed in the mycelium shape, as compared to the shake flask, as shown in Table 4. For the operation in the bioreactor, with an agitation rate of 300 rpm, the citric acid production reached 26.6 g/L, which was in excellent agreement with the results from the shake flask, where the yield of citric acid produced was 0.69 g/g of glucose utilized. This consistency between the bioreactor and shake flask results further confirms the effectiveness and reliability of the optimized conditions for citric acid production. Further analysis revealed that the optimal fermentation time for maximum citric acid production varied depending on both the organism and fermentation conditions. In this study, the highest citric acid yield (26.60 g/L) was achieved after 6 days of fermentation. Extending the fermentation period beyond this point resulted in a decline in citric acid production. This observation aligns with previous reports [28]–[31], which highlighted that extended fermentation times lead to the depletion of nitrogen and sugars in the medium, ultimately reducing citric acid yield. The findings suggest that optimizing the fermentation duration was crucial, as shorter fermentation periods yield higher citric acid concentrations while reducing the costs associated with longer fermentation times. Thus, this study not only supports the optimal fermentation parameters for citric acid production but also emphasizes the importance of controlling the fermentation duration to achieve cost-effective production at an industrial scale.

3.6 *Scanning electron microscope (SEM)*

The fermentation of *A.niger* was conducted in a 5-liter bioreactor at 30 °C with agitation set at 300 rpm. After 6 days of fermentation without pH control, as shown in Table 4, a batch fermentation process was implemented to approximate the yield range and production efficiency. The results indicated that agitation speed did not have a significant impact on the morphology of *A. niger* mycelium, which formed a single spherical pellet. In a separate bioreactor experiment with a working volume of 3 liters and 300 rpm agitation, the growth of *A. niger* mycelium was observed using scanning electron microscopy (SEM), as presented in Table 4. The images revealed no shear damage during fermentation, suggesting that the process conditions were not detrimental to mycelial integrity. The addition of $CaCl_2$ to the fermentation medium at a concentration of 0.01% significantly enhanced citric acid production. This finding was consistent with Pera & Callieri [32], who reported that the addition of 0.5 g/L $CaCl_2$ to the fermentation medium promoted citric acid production. Furthermore, the presence of Ca^{2+} induced a pelleted form of growth, characterized by highly branched hyphae and numerous bulbous cells. These bulbous cells exhibited laminated cell walls and vesicles associated with the cell wall and/or membrane, containing various inclusions, thus indicating a stimulatory effect on cellular structures and metabolic activity.

The results of the batch fermentation cycles were calculated based on biomass yield from the substrate, citric acid production from the substrate, and citric acid yield from biomass production. The citric acid production in three times of bioreactor operation were 26.88 g/L, 21.76 g/L, and 26.88 g/L, respectively. The highest citric acid yield was observed in the third batch, with a ratio of 0.25 grams of citric acid per gram of glucose. The average citric acid yield from substrate utilization was approximately 0.20 grams of citric acid per gram of glucose, highlighting the effectiveness of the fermentation conditions and the influence of $CaCl_2$ on citric acid production.

Table 4: Comparison of morphological characteristics of *A. niger* biomass growth by scanning electron microscope.

Microscopic magnification	1000x	2000x	5000x
Spores	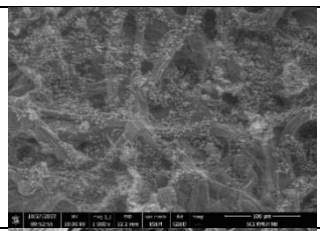	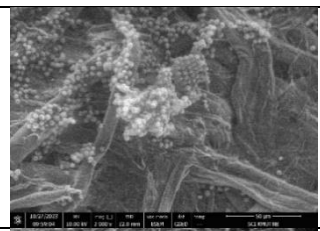	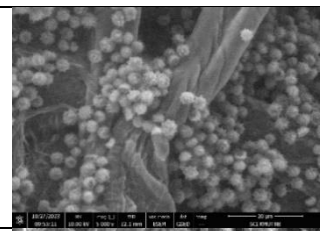
Flask	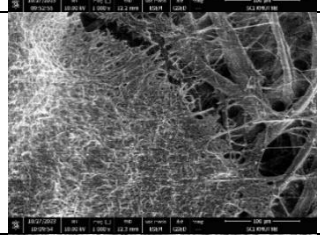	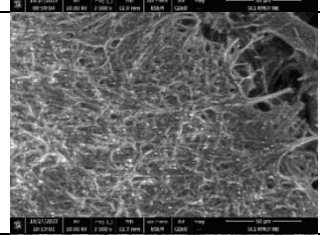	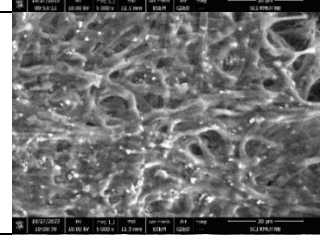
Bioreactor	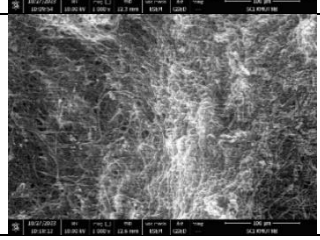	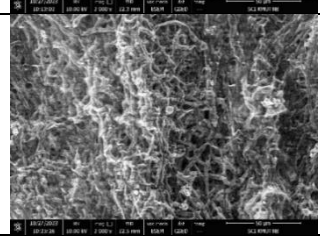	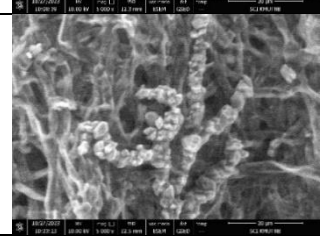

3.7 *Characterization of citric acid*

3.7.1 Fourier transform infrared spectroscopy (FT-IR)

The qualitative evaluation of citric acid (CA) in fermentation broths and commercially available citric acid (both analytical and food grades) was conducted using Fourier Transform Infrared (FTIR) spectroscopy to identify functional groups in citric acid monohydrate through characteristic absorption peaks. FTIR analysis revealed that the O-H stretching peaks in the region of approximately 3500–3000 cm^{-1} correspond to hydroxyl (O-H) stretching vibrations, originating from both carboxyl (-COOH) groups and water molecules in citric acid monohydrate. Specifically, the absorption peak at 3498 cm^{-1} corresponds to O-H stretching in anhydrous citric acid, while the peak at 3291 cm^{-1} was attributed to O-H stretching from intramolecular and intermolecular hydrogen bonding in the monohydrate form. Another important peak observed was the C=O stretching in the region of ~1750–1700 cm^{-1}, which is characteristic of carbonyl (C=O) stretching vibrations from the carboxyl (-COOH) groups in citric acid. Additionally, absorption bands in the range of ~1200–1300 cm^{-1} correspond to C-O stretching from the carboxyl group (-COOH), and C-O-C stretching in the range of ~1100-1000 cm^{-1} was attributed to ester-like stretches in the citric acid molecule [33]. When comparing citric acid monohydrate with anhydrous citric acid (without water), it was found that the FTIR spectrum of anhydrous citric acid differs significantly from that of citric acid monohydrate, primarily due to the absence of water-related peaks. Anhydrous citric acid exhibits sharper O-H stretching peaks around 3500–3000 cm^{-1} and a more defined C=O stretching peak compared to the monohydrate form. Furthermore, a weak peak around ~1650-1600 cm^{-1}, associated with water bending vibrations, was observed in the monohydrate form but absent in anhydrous citric acid.

In the FTIR analysis of citric acid derived from the fermentation of *A.niger* TISTR 2365, which underwent precipitation and crystallization, absorption peaks in the range of 3500-3200 cm^{-1} were observed, corresponding to O-H vibrations in citric acid. The peak at 3498 cm^{-1} corresponds to the free O-H group, while the peak at 3291 cm^{-1} corresponds to O-H groups involved in intermolecular bonding in citric acid monohydrate. Variations in the FTIR spectra among the samples were likely due to differences in moisture content and the presence of additional contaminants, which could generate extra

peaks in the C=O (~1700-1750 cm^{-1}) [34] and C-O (~1100-1200 cm^{-1}) regions, as shown in the overlay graphs in Figure 9. These peaks were typically less intense or absent in highly purified, food-grade citric acid.

The comparison of FTIR spectra between fermentation-derived citric acid and commercially available citric acid revealed differences in purity, residual moisture, and impurities present in the fermentation samples [35]. As a result, the FTIR spectrum of fermentation-derived citric acid exhibits distinctive features compared to the purified commercial citric acid, including less intense peaks in the carboxyl and hydroxyl regions and the presence of peaks related to contaminants in the fermentation process.

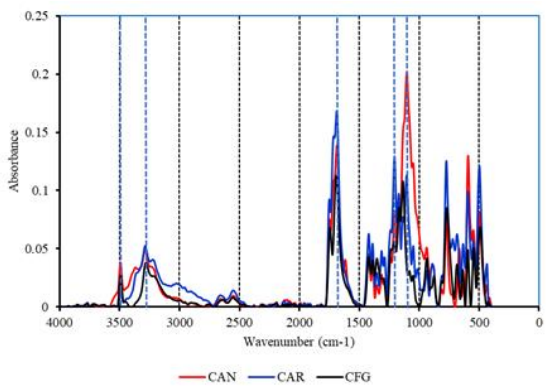

Figure 9: A comparative analysis of citric acid produced from three different sources: CAN, CAR, and CFG. The red line represents citric acid derived from *A. niger* (CAN), while the blue line corresponds to citric acid monohydrate from a commercial source (CAR) with a molecular weight of 210.14 g/mol (Sisco Research Laboratories, India). The black line represents citric acid anhydrate, a food-grade product (CFG), with a molecular weight of 192.12 g/mol (Tokyo Chemical Industry, India).

3.7.2 High-performance liquid chromatography (HPLC)

The linearity of the calibration curve (with an R-squared value of 0.9985) ensures that the relationship between peak area and citric acid concentration is highly accurate. The HPLC chromatogram in Figure 10 shows the profile of the fermentation broth. The chromatogram clearly demonstrates successful citric acid production during the fermentation process. The peak at 10.268 minutes indicated the citric acid, with the area corresponding to a concentration of 26.40 g/L. This concentration was within the expected range for citric acid production from *A. niger*, which has been optimized under specific fermentation conditions.

The presence of other smaller peaks in the chromatogram (at retention times of 7.502 min, 13.505 min, and 47.179 min) [36] suggests the production of other metabolites, which could include by-products or other organic acids, such as oxalic acid, gluconic acid, or succinic acid [37] produced during the fermentation. These metabolites may contribute to the overall metabolic profile of the *A.niger* fermentation process but were presented in lower concentrations compared to citric acid. Moreover, the concentration of citric acid (26.40 g/L) observed was significant and indicates that the fermentation conditions (including nutrient composition, agitation speed, and fermentation time) were optimized to favor citric acid production. However, the presence of by-products suggests that further optimization of the fermentation process could be done to minimize side products and maximize the yield of citric acid.

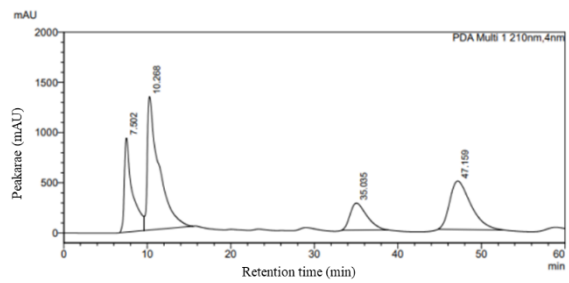

Figure 10: High Performance Liquid Chromatography (HPLC) chromatogram of fermentation broth from bioreactor by *A.niger* TISTR 2365.

4 Conclusions

The study presented in this research provides valuable insights into optimizing citric acid production through fermentation using *A.niger*. By systematically examining key fermentation parameters, including carbon to nitrogen (C/N) ratio, shaking speed and $CaCl_2$ supplementation, this work contributes to enhancing citric acid yields under controlled conditions. The use of a BBD for experimental optimization revealed a strong correlation between these factors and citric acid production, with the quadratic model showing an impressive R^2 value of 0.9866, highlighting the robustness of the optimization process. The findings align with previous studies on the metabolic versatility of *A. niger*, underscoring its importance in industrial fermentation

processes. Furthermore, the validation of the optimized conditions in both shake flask and bioreactor setups confirms the consistency and reliability of the results, demonstrating that the selected parameters are effective in improving citric acid production while maintaining mycelial integrity, as observed through scanning electron microscopy. In terms of practical application, this study not only reinforces the potential of *A.niger* in large scale citric acid production but also opens avenues for further refinement of fermentation protocols to minimize by-products and maximize yield. Moreover, the incorporation of FT-IR and HPLC analyses to characterize the citric acid produced offers an additional layer of confirmation for the product's quality, setting a foundation for future industrial applications. This method has the potential to be adapted to agricultural waste-based substrates, such as sugarcane bagasse or fruit peels, thereby enhancing sustainability and contributing to the circular bioeconomy. Overall, this work provides a comprehensive approach to optimizing citric acid production, with implications for both industrial biotechnology and microbial fermentation optimization.

Acknowledgments

This research was supported by Sweet D international company limited under Enserv Holding CO., LTD., and the Department of Biotechnology, Faculty of Applied Science, KMUTNB, for their facilities support.

Author Contributions

K.D.: conceptualization, data curation, data analysis formal analysis, methodology, research design, writing an original draft; N.P.: investigation, writing—reviewing and editing; R.R.: Investigation and manuscript preparation, including review and editing; S.K.: conceptualization, data curation, writing—reviewing and editing, funding acquisition, project administration. All authors have read and agreed to the published version of the manuscript.

Conflicts of Interest

The authors declare no conflict of interest.

References

[1] G. Perrone, G. Stea, F. Epifani, J. Varga, J. C. Frisvad, and R. A. Samson, "*Aspergillus niger* contains the cryptic phylogenetic species A. awamori," *Fungal Biology*, vol. 115, no. 11, pp. 1138–1150, Jul. 2011, doi: 10.1016/j.funbio.2011.07.008.

[2] T. C. Cairns, C. Nai, and V. Meyer, "How a fungus shapes biotechnology: 100 years of *Aspergillus niger* research," *Fungal Biology and Biotechnology*, vol. 5, no. 1, May 2018, doi: 10.1186/s40694-018-0054-5.

[3] A. Latif, N. Hassan, H. Ali, M. B. K. Niazi, Z. Jahan, I. L. Ghuman, F. Hassan, and A. Saqib, "An overview of key industrial product citric acid production by *Aspergillus niger* and its application," *Journal of Industrial Microbiology & Biotechnology*, Mar. 2025, doi: 10.1093/jimb/kuaf007.

[4] E. Książek, "Citric acid: Properties, microbial production, and applications in industries," *Molecules*, vol. 29, no. 1, p. 22, Dec. 2023, doi: 10.3390/molecules29010022.

[5] Lineback, I. J. Russell, and C. Rasmussen, "Two forms of the glucoamylase of *Aspergillus niger*," *Archives of Biochemistry and Biophysics*, vol. 134, no. 2, pp. 539–553, Nov. 1969, doi: 10.1016/0003-9861(69)90316-6.

[6] J. H. Pazur, H. R. Knull, and A. Cepure, "Glycoenzymes: Structure and properties of the two forms of glucoamylase from *Aspergillus niger*," *Carbohydrate Research*, vol. 20, no. 1, pp. 83–96, Nov. 1971, doi: 10.1016/s0008-6215(00)84951-4.

[7] A. Clarke and B. Stone, "Properties of a β-(1→4)-glucan hydrolase from *Aspergillus niger*," *Biochemical Journal*, vol. 96, no. 3, pp. 802–807, Sep. 1965, doi: 10.1042/bj0960802.

[8] R. B. Cain, "The identity of shikimate dehydrogenase and quinate dehydrogenase in *Aspergillus niger*," *Biochemical Journal*, vol. 127, no. 2, p. 15P, Apr. 1972, doi: 10.1042/bj1270015pa.

[9] H. Tsuge, O. Natsuaki, and K. Ohashi, "Purification, properties, and molecular features of glucose oxidase from *Aspergillus niger*," *The Journal of Biochemistry*, vol. 78, no. 4, pp. 835–843, Oct. 1975, doi: 10.1093/oxfordjournals.jbchem.a130974.

[10] T. Toraya, M. Fujimura, S.-I. Ikeda, S. Fukui, H. Yamada, and H. Kumagai, "Affinity chromatography of amine oxidase from *Aspergillus niger*," *Biochimica Et Biophysica Acta (BBA) - Proteins and Proteomics*, vol. 420,

no. 2, pp. 316–322, Feb. 1976, doi: 10.1016/0005-2795(76)90323-8.

[11] P. Mill, "The pectic enzymes of *Aspergillus niger*. A mercury-activated exopolygalacturonase," *Biochemical Journal*, vol. 99, no. 3, pp. 557–561, Jun. 1966, doi: 10.1042/bj0990557.

[12] K. Zhang, B. Zhang, and S. Yang, "Production of citric, itaconic, fumaric, and malic acids in filamentous fungal fermentations," *Bioprocessing Technologies in Biorefinery for Sustainable Production of Fuels, Chemicals, and Polymers*, pp. 375–398, Jul. 2013, doi: 10.1002/9781118642047.ch20.

[13] G. J. G. Ruijter, H. Panneman, and J. Visser, "Overexpression of phosphofructokinase and pyruvate kinase in citric acid-producing *Aspergillus niger*," *Biochimica Et Biophysica Acta (BBA) - General Subjects*, vol. 1334, no. 2–3, pp. 317–326, Mar. 1997, doi: 10.1016/s0304-4165(96)00110-9.

[14] N. V. Torres, "Modeling approach to control of carbohydrate metabolism during citric acid accumulation by *Aspergillus niger*: II. Sensitivity analysis," *Biotechnology and Bioengineering*, vol. 44, no. 1, pp. 112–118, Jun. 1994, doi: 10.1002/bit.260440116.

[15] L. Karaffa and C. P. Kubicek, "*Aspergillus niger* citric acid accumulation: Do we understand this well working black box?," *Applied Microbiology and Biotechnology*, vol. 61, no. 3, pp. 189–196, Jan. 2003, doi: 10.1007/s00253-002-1201-7.

[16] A. Netik, N. V. Torres, J.-M. Riol, and C. P. Kubicek, "Uptake and export of citric acid by *Aspergillus niger* is reciprocally regulated by manganese ions," *Biochimica Et Biophysica Acta (BBA) - Biomembranes*, vol. 1326, no. 2, pp. 287–294, Jun. 1997, doi: 10.1016/s0005-2736(97)00032-1.

[17] M. Papagianni, M. Mattey, M. Berovic and B. Kristiansen, "*Aspergillus niger* morphology and citric acid production in submerged batch fermentation effects of culture pH, phosphate and manganese levels," *Food Technology and Biotechnology*, vol. 37, pp. 165–171, 1999.

[18] M. Papagianni, M. Mattey, and B. Kristiansen, "The influence of glucose concentration on citric acid production and morphology of *Aspergillus niger* in batch and culture," *Enzyme and Microbial Technology*, vol. 25, no. 8–9, pp. 710–717, Nov. 1999, doi: 10.1016/s0141-0229(99)00102-7.

[19] B. Max, J. M. Salgado, N. Rodríguez, S. Cortés, A. Converti, and J. M. Domínguez, "Biotechnological production of citric acid," *Brazilian Journal of Microbiology*, vol. 41, no. 4, pp. 862–875, Aug. 2010, doi: 10.1590/s1517-83822010000400005.

[20] M. Hossain, J. D. Brooks, and I. S. Maddox, "The effect of the sugar source on citric acid production by Aspergillus niger," *Applied Microbiology and Biotechnology*, vol. 19, no. 6, pp. 393–397, Jun. 1984, doi: 10.1007/bf00454376.

[21] M. Papagianni, M. Mattey, and B. Kristiansen, "Hyphal vacuolation and fragmentation in batch and fed-batch culture of *Aspergillus niger* and its relation to citric acid production," *Process Biochemistry*, vol. 35, no. 3–4, pp. 359–366, Nov. 1999, doi: 10.1016/s0032-9592(99)00079-5.

[22] X. Yin, H.-D. Shin, J. Li, G. Du, L. Liu, and J. Chen, "Comparative genomics and transcriptome analysis of *Aspergillus niger* and metabolic engineering for citrate production," *Scientific Reports*, vol. 7, no. 1, Jan. 2017, doi: 10.1038/srep41040.

[23] B. G. Hall, "Building Phylogenetic Trees from Molecular Data with MEGA," *Molecular Biology and Evolution*, vol. 30, no. 5, pp. 1229–1235, Mar. 2013, doi: 10.1093/molbev/mst012.

[24] G. L. Miller, "Use of dinitrosalicylic acid reagent for determination of reducing sugar," *Analytical Chemistry*, vol. 31, no. 3, pp. 426–428, Mar. 1959, doi: 10.1021/ac60147a030.

[25] D. V. Guebel and N. V. T. Darias, "Optimization of the citric acid production by *Aspergillus niger* through a metabolic flux balance model," *Electronic Journal of Biotechnology*, vol. 4, no. 1, pp. 7–8, Apr. 2001, doi: 10.4067/s0717-34582001000100001.

[26] T. Eom, J. Isanapong, P. Kumnorkaew, M. Sriariyanun, and P. Pornwongthong, "1-Ethyl-3-methylimidazolium acetate pretreatment for maximizing reducing sugar recovery from mixed cabbage residue," *Environmental Science and Pollution Research*, vol. 31, no. 10, pp. 15491–15502, Feb. 2024, doi: 10.1007/s11356-024-32189-1.

[27] P. Naveen, S. Sivamani, A. Cuento, and S. Pachiyappan, "Chemical route for synthesis of citric acid from orange and grape juices," *Chemical Industry and Chemical Engineering Quarterly*, vol. 28, no. 2, pp. 135–140, Jul. 2021, doi: 10.2298/ciceq200820025n.

[28] S. Wieczorek and H. Brauer, "Continuous production of citric acid with recirculation of the fermentation broth after product recovery," *Bioprocess Engineering*, vol. 18, no. 1, p. 1, Jan. 1997, doi: 10.1007/s004490050403.

[29] J. C. Suijdam, N. W. F. Kossen, and P. G. Paul, "An inoculum technique for the production of fungal pellets," *European Journal of Applied Microbiology and Biotechnology*, vol. 10, no. 3, pp. 211–221, Jan. 1980, doi: 10.1007/bf00508608.

[30] K. Chaudary, S. Ethiraj, K. Lakshminarayana, and P. Tauro, "Citric acid production from Indian cane molasses by *Aspergillus niger* under solid state fermentation condition," *Journal of Research—Haryana Agricultural University*, vol. 1, pp. 48–52, 1978.

[31] Y. D. Hang and E. E. Woodams, "Solid state fermentation of apple pomace for citric acid production," *MIRCEN Journal of Applied Microbiology and Biotechnology*, vol. 2, no. 2, pp. 283–287, Jan. 1986, doi: 10.1007/bf00933494.

[32] L. M. Pera and D. A. Callieri, "Influence of calcium on fungal growth, hyphal morphology and citric acid production in *Aspergillus niger*," *Folia Microbiologica*, vol. 42, no. 6, pp. 551–556, Dec. 1997, doi: 10.1007/bf02815463.

[33] G. Kosa, V. Shapaval, A. Kohler, and B. Zimmermann, "FTIR spectroscopy as a unified method for simultaneous analysis of intra- and extracellular metabolites in high-throughput screening of microbial bioprocesses," *Microbial Cell Factories*, vol. 16, no. 1, Nov. 2017, doi: 10.1186/s12934-017-0817-3.

[34] A. Das, S. Bhattacharyya, R. Uppaluri, and C. Das, "Optimality of poly-vinyl alcohol/ starch/glycerol/citric acid in wound dressing applicable composite films," *International Journal of Biological Macromolecules*, vol. 155, pp. 260–272, Mar. 2020, doi: 10.1016/j.ijbiomac. 2020.03.185.

[35] Mirghani, M. E. S., & Kabbashi, N. A., "Production of citric acid from sugarcane molasses by *Aspergillus niger* using submerged fermentation: Citric acid from molasses using submerged fermentation," *Biological and Natural Resources Engineering Journal*, vol. 2, no. 1, pp. 47–55, 2019.

[36] R. Yu, J. Liu, Y. Wang, H. Wang, and H. Zhang, "*Aspergillus niger* as a Secondary Metabolite Factory," *Frontiers in Chemistry*, vol. 9, Jul. 2021, doi: 10.3389/fchem.2021.701022.

[37] X. Yin, J. Li, H.-D. Shin, G. Du, L. Liu, and J. Chen, "Metabolic engineering in the biotechnological production of organic acids in the tricarboxylic acid cycle of microorganisms: Advances and prospects," *Biotechnology Advances*, vol. 33, no. 6, pp. 830–841, Apr. 2015, doi: 10.1016/j.biotechadv.2015.04.006.